

## $\chi$ VALUES FOR BLUE EMISSION LINES IN M DWARFS

ANDREW A. WEST

Astronomy Department, University of California, Berkeley, CA and  
MIT Kavli Institute for Astrophysics and Space Research, Cambridge, MA

SUZANNE L. HAWLEY

Department of Astronomy, University of Washington, Seattle, WA  
in November 2008 issue of PASP, 120, 1161

### ABSTRACT

We compute  $\chi$  values for blue emission lines in active M dwarfs. Using flux-calibrated spectra from nearby M dwarfs and spectral M dwarf templates from SDSS, we derive analytic relations that describe how the  $\chi$  values for the CaII H and K as well as the H $\beta$ , H $\gamma$ , H $\delta$ , H $\epsilon$  and H8 Balmer emission lines vary as a function of spectral type and color. The  $\chi$  values are useful for numerous M dwarf studies where the intrinsic luminosity of emission lines cannot be estimated due to uncertain distances and/or non-flux-calibrated spectra. We use these results to estimate the mean properties of blue emission lines in active field M dwarfs from SDSS.

*Subject headings:* stars — Data Analysis and Techniques — Astronomical Techniques

### 1. INTRODUCTION

The domination of M dwarfs in the Galaxy's stellar census makes them ideal tracers of the kinematics, structure, and evolution of the Milky Way. Many of these stars are also host to large magnetic fields that act to heat the upper atmosphere and give rise to magnetic activity (as often traced by chromospheric emission lines). Observations of magnetic activity put important constraints on the internal structure, the relationship between magnetic field generation and rotation, atmospheric models, and the ages of M dwarfs. Although low-mass stars are intrinsically faint, recent large surveys include an unprecedented number of M dwarfs. The Sloan Digital Sky Survey (SDSS; Adelman-McCarthy et al. 2008) in particular has identified  $\sim 30$  million M dwarfs in the photometric database (Bochanski et al., in prep.) and over 40,000 M dwarfs with spectra (West et al. 2008). West et al. (2004, 2006) and Bochanski et al. (2007) used these spectra to statistically examine the magnetic activity properties (as traced by H $\alpha$ ) of field M dwarfs. Because the SDSS sample traces a large range of physical and dynamic properties, it provides an important laboratory for studying how magnetic activity changes as a function of mass, metallicity, rotation, and stellar age (West et al. 2008).

Magnetic activity is often quantified by computing the ratio of the luminosity in an emission line (typically H $\alpha$ ) to the bolometric luminosity of the star ( $L_{\text{H}\alpha}/L_{\text{bol}}$ ; Reid et al. 1995; Hawley et al. 1996; Burgasser et al. 2002; West et al. 2004). This quantity allows for comparison of stars of different temperatures, where changes in the continua can severely affect the derived equivalent widths. Although the activity-bolometric ratio is strictly distance independent, the challenges associated with obtaining accurate bolometric fluxes (namely good bolometric corrections for individual stars) have resulted in studies that use a color or spectral type dependent bolometric luminosity (e.g. Hawley et al. 1996), and thus

still require a distance to solve for the line emission luminosity. For H $\alpha$ , the line luminosity is often calculated using the equivalent width of the emission line, and the luminosity of the continuum near H $\alpha$ ; the latter can be measured directly from a flux-calibrated spectrum and a measured stellar distance. Alternatively, the continuum luminosity can be estimated from the photometric colors (Reid et al. 1995). Because of the difficulty in calculating individual bolometric corrections for large samples of stars, the fact that many spectra are not flux-calibrated (e.g. high resolution echelle data and data taken under non-photometric conditions) and that distance estimates to most M dwarfs are still a major source of systematic uncertainty (Covey et al. 2008), an alternative approach to calculating the activity-bolometric ratio is required.

Walkowicz et al. (2004, hereafter WHW04) and later West et al. (2005), introduced a novel method for calculating  $L_{\text{H}\alpha}/L_{\text{bol}}$  by removing many of the intermediate steps and requiring only a measurement of the equivalent width of the emission line (EW) and either the color or the spectral type of the star. WHW04, defined a sample of nearby stars with known distances (from trigonometric parallax), derived bolometric corrections and used flux-calibrated spectra to solve for the ratio of the H $\alpha$  continuum region luminosity to the bolometric luminosity as a function of both spectral type and color. This ratio is dubbed  $\chi$ ,

$$\chi = L_{\text{H}\alpha}(\text{continuum})/L_{\text{bol}}, \quad (1)$$

and when multiplied by the EW of the H $\alpha$  emission line yields the following  $L_{\text{H}\alpha}/L_{\text{bol}}$  ratio:

$$L_{\text{H}\alpha}/L_{\text{bol}} = \chi \times EW_{\text{H}\alpha} (\text{\AA}). \quad (2)$$

The power of the  $\chi$  method (WHW04) is that it does not require a flux-calibrated spectrum to obtain  $L_{\text{H}\alpha}/L_{\text{bol}}$ , and it is distance independent. Although previous studies had applied similar strategies for obtaining  $L_{\text{H}\alpha}/L_{\text{bol}}$  (Reid et al. 1995; Hawley et al. 1996; Mohanty & Basri 2003), they did not explicitly report recipes for obtaining

“ $\chi$ ” and they relied on colors and photometric or spectroscopic parallax relations, or in the latter case, spectral models, to obtain  $L_{H\alpha}(\text{continuum})$ . WHW04 was the first study to use flux-calibrated spectra to determine  $L_{H\alpha}(\text{continuum})$  and to present empirical  $\chi$  values in  $H\alpha$  for the entire M dwarf sequence.

Recently, Reiners & Basri (2008) derived  $\chi$  values for  $H\alpha$  from model spectra as a function of effective temperature. Although the Reiners & Basri (2008)  $\chi$  relations are similar to those in WHW04 for stars hotter than 2600 K ( $\sim M6$ ), they do not produce the plateau seen in the late-type empirically derived  $\chi$ s from WHW04. This discrepancy is likely due to problems with the spectral models of late-type dwarfs, which do not reproduce the correct optical colors and magnitudes of M dwarfs (Covey et al. 2008). The difference in derived  $\log(L_{H\alpha}/L_{bol})$  values using the two methods rises to 0.6 dex at a spectral type of M9. We prefer to rely on the measured data rather than models, and adopt the WHW04  $\chi$  values for  $H\alpha$  in our analysis.

The WHW04  $\chi$ s have shown great utility in computing  $L_{H\alpha}/L_{bol}$  in numerous studies (e.g., West et al. 2004; Silvestri et al. 2006; Bochanski et al. 2007; Reiners & Basri 2008), but  $H\alpha$  is not the only emission line produced by an active chromosphere. In fact,  $H\alpha$  may not always be the best tracer of activity as compared to other lines (Browning et al. 2008; Walkowicz & Hawley 2008). Traditionally, there have been several limitations in using the bluer emission lines, namely that the signal-to-noise ratio (S/N) in the blue part of an M dwarf spectrum is low because the continuum emission peaks in the near-infrared, and CCDs have been more sensitive in the red. Several recent studies have examined magnetic activity as traced by the Ca II H and K emission lines and higher order Balmer transitions including  $H\beta$ ,  $H\gamma$ ,  $H\delta$ ,  $H\epsilon$  and H8 (Rauscher & Marcy 2006; Bochanski et al. 2007; Browning et al. 2008; Walkowicz & Hawley 2008), but star-to-star comparisons have been limited by the lack of line specific  $\chi$  conversions to activity-bolometric luminosity ratios.

In this paper, we expand upon the WHW04 study, using similar methods to compute  $\chi$  values for the Ca II H and K emission lines as well as the  $H\beta$ ,  $H\gamma$ ,  $H\delta$ ,  $H\epsilon$  and H8 Balmer emission lines. We describe the data and our techniques in §2. In §3 we derive  $\chi$  for each emission line as a function of both color and spectral type and use these values to investigate the mean emission line properties of active M dwarfs. We discuss the results in §4.

## 2. DATA AND ANALYSIS

We used two complementary techniques and datasets to derive a single set of  $\chi$  values for the blue emission lines in M dwarfs. The first technique uses flux-calibrated blue spectra for a sample of nearby stars with good parallaxes and distances. The second made use of the Bochanski et al. (2007) SDSS spectral templates, which provide high S/N average spectra at each M spectral type, flux-calibrated on a relative scale. These two methods were combined to derive  $\chi$  values as a function of both color and spectral type and are described in detail below.

### 2.1. Nearby Stars with Flux-Calibrated Spectra

We used the blue spectra of 18 nearby M dwarfs from Pettersen & Hawley (1989, hereafter PH89). The observations were made using the Cassegrain spectrograph on the 2.1m Struve telescope at McDonald Observatory, with resolution  $R\sim 1,000$  and spectral range 3600-4500 Å. Our analysis used the PH89 spectra as well as a few additional unpublished spectra from the same program. Because most of the PH89 stars were observed at multiple epochs, we chose the highest S/N spectrum for each star to use in our analysis. A list of the stars and their properties can be found in Table 1. The optical and infrared photometry listed in Table 1 were compiled from Bessell (1991), Koen et al. (2002), Leggett (1992), Cutri et al. (2003, 2MASS) and SIMBAD<sup>1</sup>. The parallaxes were taken from the Hipparcos catalog (Perryman & ESA 1997). Close binary systems (Gl 473AB, Gl 644AB, Gl 234AB, Gl268AB) were not separated. Their combined spectra are ascribed to the earlier type star in the system.

Bolometric corrections for each star were computed using the  $K$ -band relations from Leggett et al. (1996, 2001) as a function of  $I - K$  colors. In two cases  $I_C$  magnitudes were not available and the  $J - K$  relations were used. All of the bolometric corrections were derived after first transforming the  $K_S$  2MASS magnitudes to  $K_{UKIRT}$  magnitudes using the Carpenter (2001) relations. Bolometric luminosities were obtained assuming  $M_{bol,\odot} = 4.64$  (Schmidt-Kaler 1982).

Continuum fluxes were measured by taking the mean continuum flux near emission lines in each spectrum. Table 2 gives the wavelength range for each continuum region. The CaII H, CaII K and  $H\epsilon$  lines have the same continuum region (as in Rauscher & Marcy 2006). The continuum fluxes were converted to luminosity using the distance to each star. By dividing the continuum luminosity by the bolometric luminosity, we calculated the  $\chi$  value for each emission line region for each star. We caution that to properly use the  $\chi$  values presented in this paper, equivalent widths should be computed using the continuum regions given in Table 2. All equivalent widths presented in this paper have been computed with these continuum regions, and users should do the same with their data.

### 2.2. Bochanski Templates

Because the PH89 spectra only include M dwarfs with spectral types M0-M5, we supplemented our analysis with the SDSS spectral templates of Bochanski et al. (2007). Bochanski et al. (2007) used over 4000 SDSS spectra to construct mean templates of M0-L0 dwarfs that have both higher S/N and higher resolution ( $R\sim 10,000$ ) than their native SDSS components. The higher resolution was achieved by using a spectral drizzle technique that involves co-adding a large number of spectra after first adjusting each spectrum to zero radial velocity on a sub-pixel grid (for more details see Bochanski et al. 2007). Although the template spectra are not on an absolute flux scale, they are on a normalized relative flux scale that is accurate to better than 4% (Bochanski et al. 2007). The templates therefore provide high S/N measurements of the continuum flux (on a relative scale) for each of the M dwarf spectral types. The tem-

<sup>1</sup> SIMBAD can be accessed online at <http://simbad.u-strasbg.fr/Simbad>.

TABLE 1  
NEARBY M DWARFS WITH BLUE SPECTRA

Name	Sp. Type	parallax (mas)	$B^a$	$V^a$	$R^a$	$I^a$	$J^b$	$H^b$	$K_S^b$
Gl 277b	M3.5	87.15	13.30	11.78	10.62	9.07	7.57	6.99	6.76
Gl 277a	M2.5	87.61	12.03	10.57	9.52	8.15	6.77	6.18	5.93
CU Cnc	M3.5	78.05	12.83	12.05	11.4	...	7.51	6.90	6.60
BD+33 1646b	M3	48.26	13.2	11.4	...	...	8.00	7.36	7.16
Gl 473AB	M5/M7	227.0	14.30	12.46	10.90	8.92	6.99	6.40	6.04
AD Leo	M3	213.0	10.85	9.32	8.23	6.81	5.45	4.84	4.59
DT Vir	M0.5	87.50	11.23	9.76	8.81	7.71	6.44	5.79	5.58
Gl 490A	M0.5	55.27	12.2	10.5	9.73	8.8	7.40	6.73	6.55
Gl 725B	M3.5	284.48	11.47	9.69	8.56	7.13	5.72	5.20	5.00
CE Boo	M2.5	101.91	11.68	10.2	9.4	8.5	6.63	5.99	5.77
Gl 644AB	M3/M4	174.22	10.60	9.02	7.92	6.55	5.27	4.78	4.40
Gl 725A	M3	280.28	10.44	8.90	7.83	6.44	5.19	4.74	4.43
Gl 182	M0.5	37.50	11.48	10.07	9.18	8.24	7.12	6.45	6.26
Gl 234AB	M4.5/M8	242.88	12.80	11.08	9.77	8.06	8.10	7.47	7.21
Gl 268AB	M4.5/M6	157.23	13.19	11.49	10.16	8.44	6.73	6.15	5.85
YZ CMi	M4.5	168.59	12.76	11.15	9.89	8.2	6.58	6.01	5.70
CW UMa	M3.5	68.3	14.02	12.38	11.2	9.7	8.30	7.76	7.50
Gl 685	M0.5	70.95	11.45	9.97	9.2	8.3	6.88	6.27	6.07

NOTE. — M dwarfs from the spectroscopic sample of Pettersen & Hawley (1989)

<sup>a</sup>Optical photometry from Bessell (1991), Koen et al. (2002), Leggett (1992) and SIMBAD

<sup>b</sup>IR photometry from 2MASS (Cutri et al. 2003)

TABLE 2  
CONTINUUM REGIONS

Emission Line	Region 1 (Å)	Region 2 (Å)
H $\alpha$	6555-6560	6570-6575
H $\beta$	4840-4850	4875-4885
H $\gamma$	4310-4330	4350-4370
H $\delta$	4075-4095	4110-4130
H8	3865-3885	3895-3915
CaII K/CaII H/He	3974-3976	3952.7-3956

plates are further divided into categories of H $\alpha$  activity. We examined the active and inactive templates at each spectral type and found no continuum variation in the active versus inactive spectra. We therefore chose to use the combined (active plus inactive) templates for our  $\chi$  analysis.

We measured the continuum region around the H $\alpha$  emission line at each spectral type (see Table 2) and used the  $\chi$  values from WHW04 to calibrate each template spectrum to units of  $L/L_{bol}$ . We measured the continuum regions around each emission line for all of the templates in the same manner as the PH89 spectra. Because of the WHW04 calibration, the mean continuum values are direct measurements of  $\chi$ . Uncertainties in the  $\chi$  values were computed from the spread of the composite spectra used to create the Bochanski et al. (2007) templates.

### 3. RESULTS

The resulting  $\chi$  values are shown as a function of spectral type in Figure 1. The H $\alpha$  values (upper-left; triangles) are from the WHW04 study. Asterisks denote the  $\chi$  values derived from the Bochanski templates, and diamonds show the  $\chi$  values computed from the nearby blue spectra. There is excellent agreement between the two different methods. Table 3 gives the mean  $\chi$  values as a

function of spectral type with uncertainties representing the spread of  $\chi$  at each spectral type (in parentheses). Interestingly, Figure 1 shows a plateau in  $\chi$  values over the spectral type range M7-L0 in every emission line for which we have data. This was previously seen, though not discussed, in WHW04 for H $\alpha$ . This striking feature is evidently produced by a balance between the decreasing temperature (bolometric luminosity) and decreasing optical continuum flux in these late-type dwarfs. We note again that these empirical results disagree with the Reiners & Basri (2008) values derived using model spectra, which we attribute to deficiencies in the models. The details of this plateau are left for future analysis.

Figures 2-4 show the  $\chi$  values as a function of  $i - z$ ,  $i - J$ , and  $V - I$  colors. For the  $i - z$  and  $i - J$  relations, we transformed from spectral type to color using the mean  $i - z$  and  $i - J$  colors for M dwarfs reported by West et al. (2008). The  $V - I$  vs.  $\chi$  relations for H $\gamma$ , H $\delta$ , H8, along with the CaIIK, CaIIH, and H $\epsilon$ , were obtained using the observed colors of the individual nearby stars in PH89 (see Table 1) and the measured  $\chi$  values discussed above, while the H $\alpha$  relation is taken from the colors and  $\chi$  values in WHW04. The colors for the H $\beta$   $V - I$  versus  $\chi$  relation were derived by transforming the mean  $i - z$  colors for each spectral type to  $V - I$  using the  $r - i$  vs.  $V - I$  transformation of Davenport et al. (2006) and the following linear transformation between  $r - i$  and  $i - z$  that we found from the West et al. (2008) sample:

$$i - z = 0.54(r - i) + 0.01. \quad (3)$$

The  $V - I$  vs.  $\chi$  relations do not extend beyond  $V - I > 3.05$  ( $\sim$ M5; except for H $\alpha$ ) due to the lack of late-type M dwarfs with measured  $V - I$  colors in the PH89 sample.

We fit analytic relations to our derived  $\chi$  values as a function of spectral type,  $i - z$ ,  $i - J$  and  $V - I$  color. We adopt the exponential form of WHW04:

$$\chi = ae^{-V/b} + c, \quad (4)$$

TABLE 3  
 $\chi$  VALUES

Sp. Type	$\chi_{H\alpha}$ ( $\times 10^{-4}$ ) <sup>a</sup>	$\chi_{H\beta}$ ( $\times 10^{-4}$ )	$\chi_{H\gamma}$ ( $\times 10^{-4}$ )	$\chi_{H\delta}$ ( $\times 10^{-4}$ )	$\chi_{H8}$ ( $\times 10^{-4}$ )	$\chi_{CaIK/CaIH/He\epsilon}$ ( $\times 10^{-4}$ ) <sup>b</sup>
M0	1.160 (0.277)	0.600 (0.143)	0.253 (0.090)	0.185 (0.067)	0.082 (0.029)	0.102 (0.041)
M1	1.160 (0.451)	0.484 (0.187)	0.238 (0.077)	0.174 (0.056)	0.078 (0.024)	0.098 (0.036)
M2	0.966 (0.306)	0.349 (0.111)	0.146 (0.038)	0.117 (0.031)	0.054 (0.018)	0.072 (0.021)
M3	0.738 (0.216)	0.235 (0.069)	0.082 (0.034)	0.069 (0.027)	0.033 (0.015)	0.044 (0.016)
M4	0.637 (0.286)	0.167 (0.075)	0.061 (0.021)	0.051 (0.017)	0.027 (0.010)	0.036 (0.012)
M5	0.274 (0.128)	0.066 (0.031)	0.042 (0.031)	0.036 (0.023)	0.025 (0.013)	0.030 (0.016)
M6	0.176 (0.052)	0.034 (0.010)	0.011 (0.003)	0.009 (0.003)	0.007 (0.002)	0.010 (0.003)
M7	0.052 (0.015)	0.008 (0.002)	0.002 (0.001)	0.002 (0.001)	0.002 (0.001)	0.002 (0.001)
M8	0.060 (0.029)	0.008 (0.004)	0.002 (0.002)	0.002 (0.002)	0.005 (0.004)	0.001 (0.002)
M9	0.038 (0.011)	0.005 (0.002)	0.002 (0.001)	0.001 (0.001)	0.003 (0.004)	... ( ... )
L0	0.047 (0.007)	0.007 (0.003)	0.001 (0.001)	... ( ... )	... ( ... )	... ( ... )

NOTE. — Uncertainties derived from the spread in  $\chi$  are given in parentheses.

<sup>a</sup> $H\alpha$   $\chi$  values computed from WHW04.

<sup>b</sup>The  $\chi$  values for CaII K, CaII H and He are the same because the continuum regions used to compute the equivalent widths are the same for all three lines.

TABLE 4  
 $\chi$  VS. SPECTRAL TYPE

$\chi$	a	b	c	Range	$\sigma\chi$
$\chi_{H\alpha}$	0.54186	$3.33 \times 10^4$	-0.54173	M0-M5.5 (0-5.5)	$3.31 \times 10^{-5}$
$\chi_{H\alpha}$	0.193	0.621	$4.92 \times 10^{-6}$	M5.5-L0 (5.5-10)	$4.55 \times 10^{-6}$
$\chi_{H\beta}$	$9.49 \times 10^{-5}$	6.21	$-3.39 \times 10^{-5}$	M0-M6.5 (0-6.5)	$3.17 \times 10^{-6}$
$\chi_{H\beta}$	$1.37 \times 10^{-5}$	1.80	$5.39 \times 10^{-7}$	M6.5-L0 (6.5-10)	$2.25 \times 10^{-7}$
$\chi_{H\gamma}$	$3.42 \times 10^{-5}$	3.04	$-3.50 \times 10^{-6}$	M0-M6.5 (0-6.5)	$2.14 \times 10^{-5}$
$\chi_{H\gamma}$	$1.64 \times 10^6$	0.22	$1.73 \times 10^{-7}$	M6.5-M9 (6.5-9)	$2.00 \times 10^{-7}$
$\chi_{H\delta}$	$2.65 \times 10^{-5}$	3.84	$-4.47 \times 10^{-6}$	M0-M6.5 (0-6.5)	$1.63 \times 10^{-5}$
$\chi_{H\delta}$	$4.63 \times 10^{-4}$	$1.52 \times 10^4$	$-4.619 \times 10^{-4}$	M6.5-M9 (6.5-9)	$2.00 \times 10^{-7}$
$\chi_{H8}$	$1.11 \times 10^{-5}$	4.01	$-1.329 \times 10^{-6}$	M0-M5.5 (0-5.5)	$8.31 \times 10^{-6}$
$\chi_{H8}$	$6.448 \times 10^{-4}$	0.91	$-1.26 \times 10^{-7}$	M5.5-M7 (5.5-7)	$1.38 \times 10^{-6}$
$\chi_{CaIK/CaIH/He\epsilon}$	$1.334 \times 10^{-5}$	3.82	$-1.124 \times 10^{-6}$	M0-M5 (0-5)	$1.07 \times 10^{-5}$
$\chi_{CaIK/CaIH/He\epsilon}$	$5.233 \times 10^{-5}$	1.77	$-7.629 \times 10^{-7}$	M5-M7 (5-7)	$8.95 \times 10^{-7}$

NOTE. — Coefficients for calculating  $\chi$  as a function of spectral type using the equation  $\chi = ae^{-SpT/b} + c$ . Spectral types are specified by integer values from M0=0 to L0=10.

where  $a$ ,  $b$  and  $c$  are derived coefficients and  $V$  is the associated variable (e.g.  $i - z$ ,  $i - J$ ). All of the fits were performed using a Levenberg-Marquardt least-squares method. Tables 4-7 give the resulting fit coefficients for each  $\chi$  value. Most of the fits require 2 piecewise (but continuous) components; the tables specify the range over which each fit component is valid. In addition, the tables provide a typical uncertainty in the derived  $\chi$  for each fit component.

Using our derived  $\chi$  values and the active templates of Bochanski et al. (2007), we next computed  $L_{line}/L_{bol}$  values as a function of spectral type for the  $H\alpha$ ,  $H\beta$ ,  $H\gamma$ , H8 and CaII K emission lines. The Bochanski et al. (2007) active templates consist of the mean spectrum of up to several hundred active SDSS M dwarfs at each spectral type. We measured the EWs of the  $H\alpha$ ,  $H\beta$ ,  $H\gamma$ , H8 and CaII K emission lines in each of the Bochanski et al. (2007) active templates, taking care to use the continuum regions from Table 2 for our measurements (see Section 2.1). Lines which were not in emission in a given template were omitted. Combining the measured EWs with our new  $\chi$  values gives  $L_{line}/L_{bol}$  values at each spectral type for each line. These represent the average values of

active field M dwarfs measured by SDSS.

Figure 5 shows the new activity relations, which represent the mean luminosity fractions of six different activity-tracing emission lines for thousands of active field M dwarfs. The relations suggest that the fraction of the bolometric luminosity that is produced in a given emission line increases monotonically with wavelength at all spectral types. In addition, the newly measured emission lines are consistent with the  $H\alpha$  study of West et al. (2004) that showed a constant value for  $L_{H\alpha}/L_{bol}$  for early-mid M types (M0-M4) with a decrease occurring near spectral type  $\sim$ M5. The  $L_{CaIK}/L_{bol}$  relation shown here agrees with  $L_{CaIK}/L_{bol}$  results for the  $H\alpha$  active M dwarfs from Browning et al. (2008).

#### 4. DISCUSSION

The  $\chi$  values from WHW04 provide a distance-independent way to compare the  $H\alpha$  activity of stars with different spectral types. We used a spectroscopic sample of nearby M dwarfs from Pettersen & Hawley (1989) and the Bochanski et al. (2007) templates to expand the  $\chi$  values to include the  $H\beta$ ,  $H\gamma$ ,  $H\delta$ ,  $He$ , H8, CaII K, and CaII H emission lines. We fit analytic relations to all

TABLE 5  
 $\chi$  vs.  $i - z$

$\chi$	a	b	c	Range	$\sigma\chi$
$\chi_{H\alpha}$	$2.92 \times 10^{-4}$	1.19	$-8.96 \times 10^{-5}$	0.38-1.37	$1.31 \times 10^{-5}$
$\chi_{H\alpha}$	0.011788	$4.66 \times 10^3$	$-1.1779 \times 10^{-2}$	1.37-1.84	$1.32 \times 10^{-6}$
$\chi_{H\beta}$	$2.02 \times 10^{-4}$	0.324	$-1.86 \times 10^{-6}$	0.38-1.37	$2.68 \times 10^{-6}$
$\chi_{H\beta}$	$2.378 \times 10^{-4}$	$4.61 \times 10^2$	$-2.363 \times 10^{-4}$	1.37-1.84	$2.15 \times 10^{-7}$
$\chi_{H\gamma}$	$1.62 \times 10^{-4}$	0.252	$-1.38 \times 10^{-7}$	0.38-1.10	$1.61 \times 10^{-6}$
$\chi_{H\gamma}$	$1.76 \times 10^2$	0.061	$1.72 \times 10^{-7}$	1.10-1.76	$2.00 \times 10^{-7}$
$\chi_{H\delta}$	$9.17 \times 10^{-5}$	0.311	$-9.58 \times 10^{-7}$	0.38-1.37	$6.68 \times 10^{-7}$
$\chi_{H\delta}$	$2.366 \times 10^{-4}$	$1.53 \times 10^3$	$-2.362 \times 10^{-4}$	1.37-1.76	$2.00 \times 10^{-7}$
$\chi_{H8}$	$3.02 \times 10^{-5}$	0.473	$-1.64 \times 10^{-6}$	0.38-1.37	$8.38 \times 10^{-7}$
$\chi_{CaIHK/CaIHH/He}$	$4.31 \times 10^{-5}$	0.385	$-1.07 \times 10^{-6}$	0.38-1.37	$4.87 \times 10^{-7}$

NOTE. — Coefficients for calculating  $\chi$  as a function of  $i - z$  color using the equation  $\chi = ae^{-(i-z)/b} + c$ .

TABLE 6  
 $\chi$  vs.  $i - J$

$\chi$	a	b	c	Range	$\sigma\chi$
$\chi_{H\alpha}$	$5.25 \times 10^{-4}$	1.53	$-6.09 \times 10^{-5}$	1.61-3.22	$1.29 \times 10^{-5}$
$\chi_{H\alpha}$	$2.257 \times 10^{-3}$	$2.01 \times 10^3$	$-2.248 \times 10^{-3}$	3.22-4.29	$1.33 \times 10^{-6}$
$\chi_{H\beta}$	$1.79 \times 10^{-3}$	0.477	$-8.18 \times 10^{-7}$	1.61-3.22	$2.75 \times 10^{-6}$
$\chi_{H\beta}$	$6.46 \times 10^{-6}$	1.14	$4.36 \times 10^{-7}$	3.22-4.29	$2.21 \times 10^{-7}$
$\chi_{H\gamma}$	$2.72 \times 10^{-3}$	0.370	$3.03 \times 10^{-7}$	1.61-2.85	$1.58 \times 10^{-6}$
$\chi_{H\gamma}$	$2.71 \times 10^5$	0.108	$1.70 \times 10^{-7}$	2.85-4.01	$2.00 \times 10^{-7}$
$\chi_{H\delta}$	$8.83 \times 10^{-4}$	0.460	$-5.47 \times 10^{-7}$	1.61-3.22	$6.06 \times 10^{-7}$
$\chi_{H\delta}$	$1.33085 \times 10^{-3}$	$1.73 \times 10^4$	$-1.3304 \times 10^{-3}$	3.22-4.01	$2.00 \times 10^{-7}$
$\chi_{H8}$	$1.37 \times 10^{-4}$	0.685	$-1.19 \times 10^{-6}$	1.61-3.22	$8.61 \times 10^{-7}$
$\chi_{CaIHK/CaIHH/He}$	$2.74 \times 10^{-4}$	0.563	$-6.85 \times 10^{-7}$	1.61-3.22	$4.10 \times 10^{-7}$

NOTE. — Coefficients for calculating  $\chi$  as a function of  $i - J$  color using the equation  $\chi = ae^{-(i-J)/b} + c$ .

of the  $\chi$  values (including  $H\alpha$ ) as a function of spectral type and color ( $i - z$ ,  $i - J$ , and  $V - I$ ). The new  $\chi$  values are useful for analyzing both past and future M dwarf data. Magnetic activity can be easily quantified if studies include EW measurements (measured using the continuum regions given in Table 2) and either spectral types or colors.

We show that the percentage of bolometric luminosity emitted in the optical emission lines of active-field M dwarfs increases monotonically with increasing wavelength. In addition, the emission line luminosities relative to the bolometric luminosities are constant in all measured lines for spectral types M0-M4, and then decrease at later spectral types, in agreement with the  $H\alpha$  results in West et al. (2004). The  $L_{CaIHK}/L_{bol}$  values are consistent with those measured for the  $H\alpha$  active stars from Browning et al. (2008). Unfortunately, the  $H\alpha$  inactive templates of Bochanski et al. (2007) do not have a sufficient S/N at each spectral type to systematically compare the strength of the CaII K emission lines in active and inactive stars. However, a CaII K emission line is present in the M5 inactive template. The resulting

mean  $L_{CaIHK}/L_{bol}$  for the inactive template is an order of magnitude lower than the ( $H\alpha$ ) active template.

Our  $\chi$  values have already proven useful in the rotation-activity analysis of Browning et al. (2008) by allowing  $L_{CaIHK}/L_{bol}$  and  $L_{CaIHH}/L_{bol}$  to be computed from echelle spectra. Future improvements to our  $\chi$  measurements can be made by creating a larger spectroscopic sample of nearby M dwarfs with good parallaxes. The advent of synoptic telescopes like Pan-STARRS, LSST and SIM will measure parallaxes for thousands of M dwarfs, many of which will have SDSS (or other previously observed) spectra. These samples will enable tighter constraints on  $\chi$  and better inform our understanding of magnetic activity in the majority of stellar inhabitants of the Galaxy.

The authors thank Matthew Browning, Gibor Basri, Lucianne Walkowicz, Ansgar Reiners, and John Bochanski for many fruitful conversations and suggestions that greatly improved the quality of this manuscript.

REFERENCES

Adelman-McCarthy, J. K., et al. 2008, ApJS, 175, 297  
 Bessell, M. S. 1991, AJ, 101, 662  
 Bochanski, J. J., West, A. A., Hawley, S. L., & Covey, K. R. 2007, AJ, 133, 531  
 Browning, M. K., Basri, G., Marcy, G. W., West, A. A., & Zhang, J. 2008, ApJ, submitted  
 Burgasser, A. J., Liebert, J., Kirkpatrick, J. D., & Gizis, J. E. 2002, AJ, 123, 2744

TABLE 7  
 $\chi$  vs.  $V - I$

$\chi$	a	b	c	Range	$\sigma\chi$
$\chi_{H\alpha}$	$1.92 \times 10^{-2}$	0.345	$6.36 \times 10^{-5}$	2.01-2.84	$1.54 \times 10^{-5}$
$\chi_{H\alpha}$	$4.87 \times 10^{-4}$	2.07	$-5.25 \times 10^{-5}$	2.84-4.33	$1.63 \times 10^{-5}$
$\chi_{H\beta}$	$3.12 \times 10^{-4}$	3.15	$-1.14 \times 10^{-4}$	1.67-3.05	$2.71 \times 10^{-6}$
$\chi_{H\gamma}$	$8.38 \times 10^{-5}$	1.49	$-6.74 \times 10^{-6}$	1.67-3.05	$1.62 \times 10^{-5}$
$\chi_{H\delta}$	$5.42 \times 10^{-5}$	1.83	$-6.70 \times 10^{-6}$	1.67-3.05	$1.17 \times 10^{-5}$
$\chi_{H8}$	$2.08 \times 10^{-5}$	1.83	$-1.89 \times 10^{-6}$	1.67-3.05	$5.30 \times 10^{-6}$
$\chi_{CaIIK/CaIII/H\epsilon}$	$2.36 \times 10^{-5}$	2.26	$-3.21 \times 10^{-6}$	1.67-3.05	$7.45 \times 10^{-6}$

NOTE. — Coefficients for calculating  $\chi$  as a function of  $V - I$  color using the equation  $\chi = ae^{-(V-I)/b} + c$ .

- Carpenter, J. M. 2001, AJ, 121, 2851  
Covey, K. R., et al. 2008, AJ, 136, 1778  
Cutri, R. M., et al. 2003, 2MASS All Sky Catalog of point sources. (The IRSA 2MASS All-Sky Point Source Catalog, NASA/IPAC Infrared Science Archive. <http://irsa.ipac.caltech.edu/applications/Gator/>)  
Davenport, J. R. A., West, A. A., Matthiesen, C. K., Schmieding, M., & Kobelski, A. 2006, PASP, 118, 1679  
Hawley, S. L., Gizis, J. E., & Reid, I. N. 1996, AJ, 112, 2799  
Koen, C., Kilkenny, D., van Wyk, F., Cooper, D., & Marang, F. 2002, MNRAS, 334, 20  
Leggett, S. K. 1992, ApJS, 82, 351  
Leggett, S. K., Allard, F., Berriman, G., Dahn, C. C., & Hauschildt, P. H. 1996, ApJS, 104, 117  
Leggett, S. K., Allard, F., Geballe, T. R., Hauschildt, P. H., & Schweitzer, A. 2001, ApJ, 548, 908  
Mohanty, S., & Basri, G. 2003, ApJ, 583, 451  
Perryman, M. A. C., & ESA, eds. 1997, ESA Special Publication, Vol. 1200, The HIPPARCOS and TYCHO catalogues. Astrometric and photometric star catalogues derived from the ESA HIPPARCOS Space Astrometry Mission  
Pettersen, B. R., & Hawley, S. L. 1989, A&A, 217, 187  
Rauscher, E., & Marcy, G. W. 2006, PASP, 118, 617  
Reid, N., Hawley, S. L., & Mateo, M. 1995, MNRAS, 272, 828  
Reiners, A., & Basri, G. 2008, ApJ, 684, 1390  
Schmidt-Kaler, T. 1982, Physical Properties of Stars (Landolt-Bornstein Numerical Data and Functional Relationships in Science and Technology, New Series, Group VI, Volume 2b, Springer-Verlag, Berlin)  
Silvestri, N. M., et al. 2006, AJ, 131, 1674  
Walkowicz, L. M., & Hawley, S. L. 2008, ApJ, submitted  
Walkowicz, L. M., Hawley, S. L., & West, A. A. 2004, PASP, 116, 1105  
West, A. A., Bochanski, J. J., Hawley, S. L., Cruz, K. L., Covey, K. R., Silvestri, N. M., Reid, I. N., & Liebert, J. 2006, AJ, 132, 2507  
West, A. A., Hawley, S. L., Bochanski, J. J., Covey, K. R., Reid, I. N., Dhital, S., Hilton, E. J., & Masuda, M. 2008, AJ, 135, 785  
West, A. A., Walkowicz, L. M., & Hawley, S. L. 2005, PASP, 117, 706  
West, A. A., et al. 2004, AJ, 128, 426

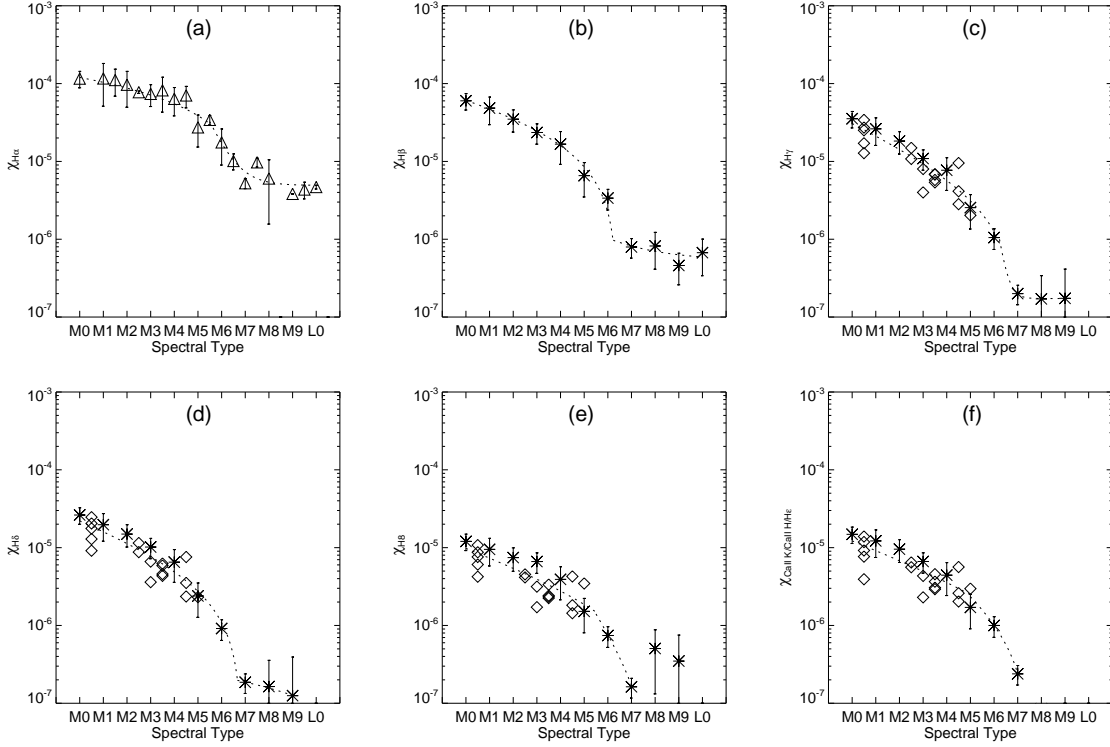


FIG. 1.—  $\chi$  as a function of spectral type for the (a)  $H\alpha$ , (b)  $H\beta$ , (c)  $H\gamma$ , (d)  $H\delta$ , (e)  $H8$ , and (f)  $H\epsilon$ , CaII H and CaII K emission lines. The  $\chi$  values were derived using results from the study of WHW04 (triangles;  $H\alpha$ ), the Bochanski et al. (2007) SDSS spectral templates (asterisks), and the flux-calibrated spectra of nearby stars (PH89; diamonds). An empirical relation (dotted lines) for each  $\chi$  value can be found using the coefficients in Table 4.

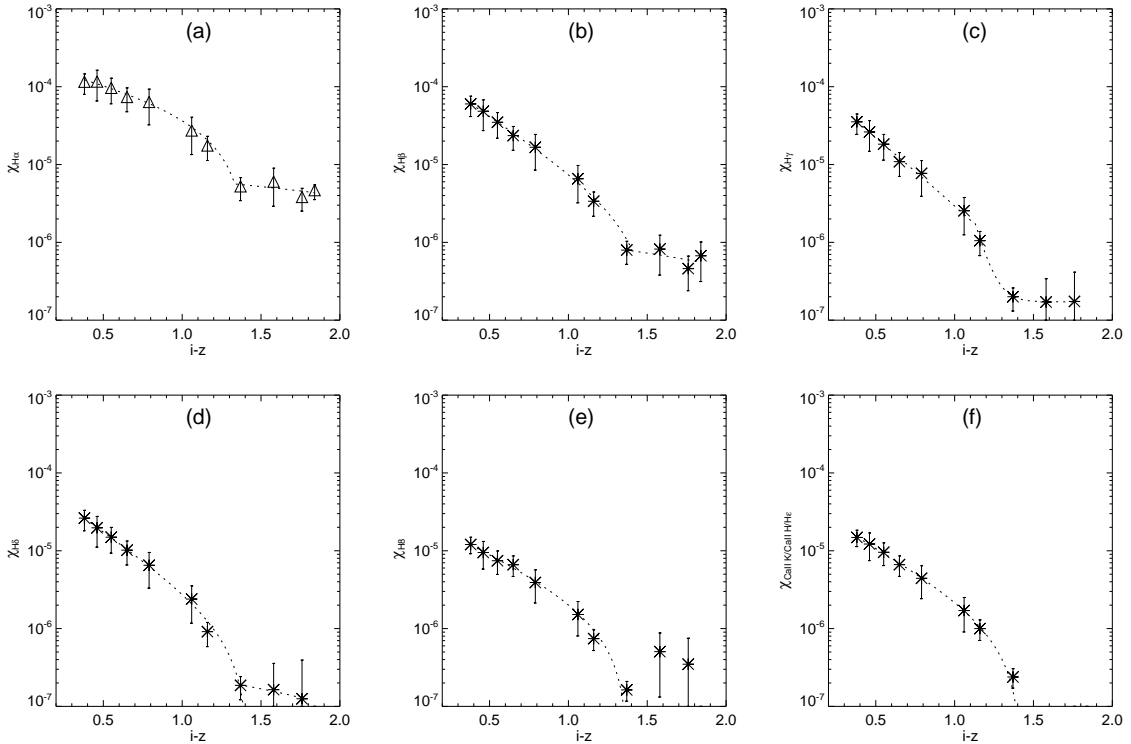


FIG. 2.—  $\chi$  as a function of  $i-z$  color for the (a)  $H\alpha$ , (b)  $H\beta$ , (c)  $H\gamma$ , (d)  $H\delta$ , (e)  $H8$ , and (f)  $H\epsilon$ , CaII H and CaII K emission lines. The  $\chi$  values were derived from the study of WHW04 (triangles;  $H\alpha$ ) and the SDSS spectral templates of (Bochanski et al. 2007, asterisks). An empirical relation (dotted lines) for each  $\chi$  value can be found using the coefficients in Table 5.

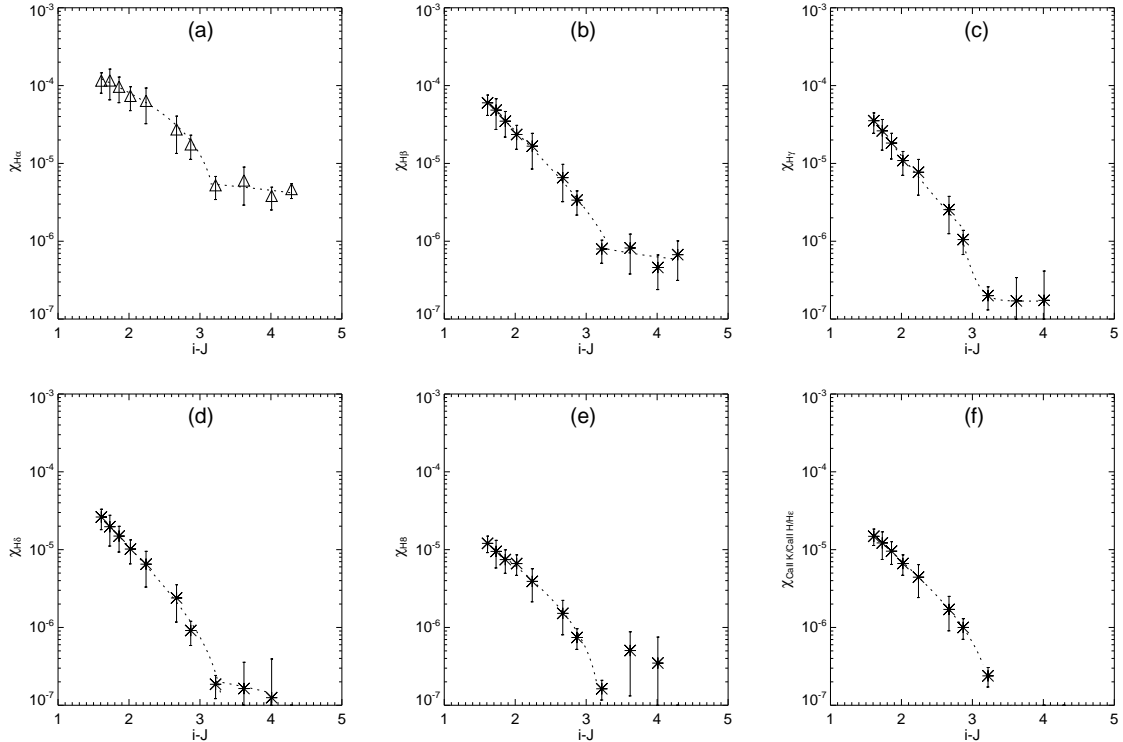


FIG. 3.—  $\chi$  as a function of  $i - J$  color for the (a)  $H\alpha$ , (b)  $H\beta$ , (c)  $H\gamma$ , (d)  $H\delta$ , (e)  $H8$ , and (f)  $H\epsilon$ , CaII H and CaII K emission lines. The  $\chi$  values were derived from the study of WHW04 (triangles;  $H\alpha$ ) and the spectral templates of Bochanski et al. (2007, asterisks). An empirical relation (dotted lines) for each  $\chi$  value can be found using the coefficients in Table 6.

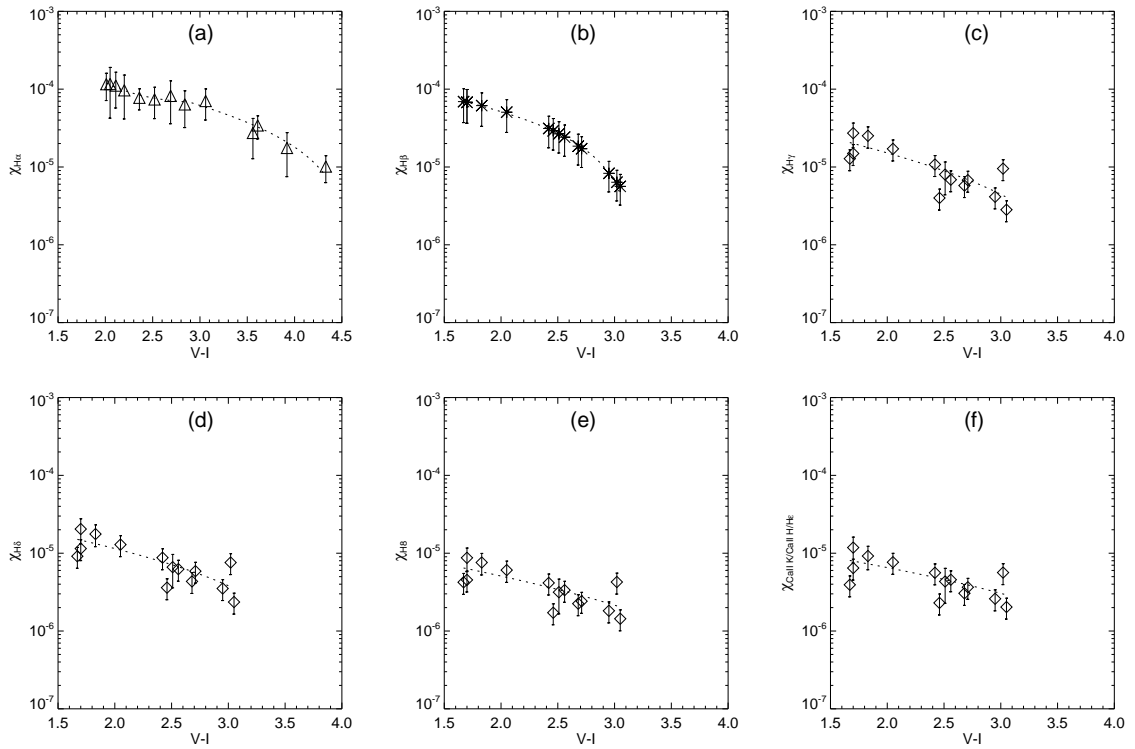


FIG. 4.—  $\chi$  as a function of  $V - I$  color for the (a)  $H\alpha$ , (b)  $H\beta$ , (c)  $H\gamma$ , (d)  $H\delta$ , (e)  $H8$ , and (f)  $H\epsilon$ , CaII H and CaII K emission lines. The  $\chi$  values were derived from the study of WHW04 (triangles;  $H\alpha$ ), the spectral templates of Bochanski et al. (2007, asterisks,  $H\beta$ ), and the flux-calibrated spectra of nearby stars (PH89; diamonds). An empirical relation (dotted lines) for each  $\chi$  value can be found using the coefficients in Table 7.



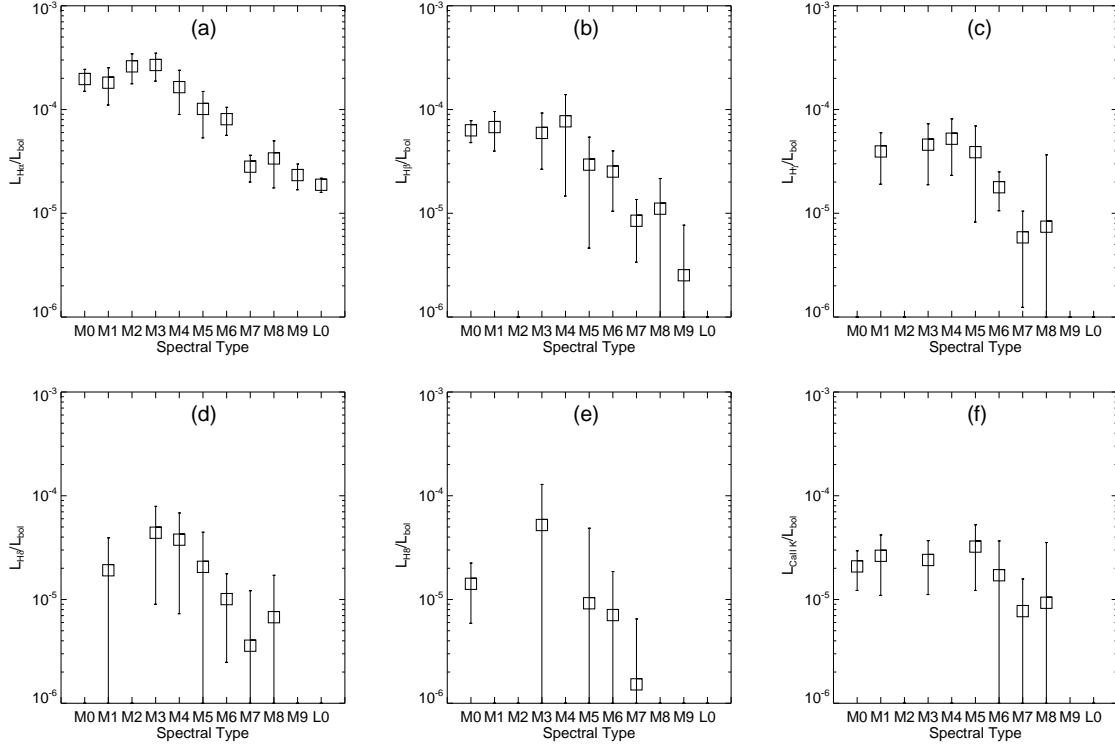


FIG. 5.—  $L_{line}/L_{bol}$  as a function of spectral type for the (a)  $H\alpha$ , (b)  $H\beta$ , (c)  $H\gamma$ , (d)  $H\delta$ , (e)  $H8$ , and (f)  $CaII\ K$  emission lines. These values were computed using equivalent width measurements from the median composite active SDSS template spectra of Bochanski et al. (2007) and the  $\chi$  values presented in this paper. The relations show that the fraction of the bolometric luminosity that is produced in a given emission line increases monotonically with wavelength at all spectral types. Also, all relations are consistent with the  $H\alpha$  study of West et al. (2004) that showed a constant  $L_{H\alpha}/L_{bol}$  value from M0-M4 with a decrease occurring at a spectral type  $\sim M5$ . In addition, the  $L_{CaIIK}/L_{bol}$  relation traces the  $L_{CaIIK}/L_{bol}$  found for  $H\alpha$  active M dwarfs in Browning et al. (2008).